BioChip J. (2011) 5(4): 343-352
DOI 10.1007/s13206-011-5408-5

Original Research

Droplet routing in high-level synthesis of configurable digital microfluidic biochips based on microelectrode dot array architecture

Zhongkai Chen[1], Daniel Hsiang-Yung Teng[2], Gary Chung-Jhih Wang[1] & Shih-Kang Fan[3]

Received: 17 August 2011 / Accepted: 27 September 2011 / Published online: 20 December 2011

Abstract Droplet-based digital microfluidic lab-on-chips exploiting electrowetting-on-dielectric (EWOD) have been studied over the last decade. With the recent introduction of new highly scalable, reconfigurable and field-programmable microelectrode dot array (MEDA) architecture, there is a compelling need for a new digital microfluidics synthesizer for the new MEDA architecture. Droplet routing is a critical part of the digital microfluidics synthesizer. This paper presents a routing algorithm and the associated performance analysis results. The algorithm is able to route different sizes of reagent and sample droplets simultaneously and also incorporates other characteristics such as diagonal movements and channel-based movements that are specific to the MEDA architecture.

Keywords: Digital microfluidics, Microelectrode dot array, Electrowetting-on-dielectric (EWOD), Droplet routing, Biochip synthesis, Lab-on-a-chip (LOC)

Introduction

Microfluidics has been defined as "the science and technology of systems that process or manipulate small amounts of fluids, using channels with dimensions of tens to hundreds of micrometers"[1]. With the development of digital microfluidics technology, multiple micro- or nano-liter droplets can be manipulated in open channels using a variety of approaches[2]. Electrowetting-on-dielectric (EWOD) is one of the most commonly used electrokinetic methods for manipulating microfluidic droplets through the modulation of interfacial tension between a conducting droplet and a solid electrode. By activating individually controlled electrodes, droplets can be moved from an electrode to its adjacent electrode. Other microfluidic operations such as dispensing, splitting, and merging of droplets are also possible with EWOD[3,4]. The capability of parallel manipulation of multiple droplets, together with design portability and precision, fosters the possibility of concurrent chemical or biological analyses on a single digital microfluidic biochip (DMFB) system.

To accommodate the anticipated increase in complexity of droplet manipulations, an innovative DMFB platform architecture, referred to as Microelectrode Dot Array (MEDA) architecture, was recently proposed[5]. In addition to improved scalability, configurability and portability, the MEDA architecture has a good potential to achieve precise and flexible control of multiple droplets concurrently (See Figure 1). However, these advantageous features of the new architecture also imposed challenges on droplet routing. As the existing droplet routing algorithms are not applicable to MEDA architecture, development of a new droplet router is essential for continuing study of MEDA architecture.

Compared to traditional DMFB architecture, the complexity of routing for MEDA architecture is expected to be greatly increased due to concurrent move-

[1]University of Saskatchewan, Saskatoon, SK. S7N 5A9 Canada
[2]Electrical and Computer Engineering Department, University of Saskatchewan, Saskatoon, SK. S7N 5A9 Canada
[3]Materials Science and Engineering Department, National Chiao Tung University, Hsinchu, Taiwan
Correspondence and requests for materials should be addressed to D.H.-Y. Teng (✉d.teng@usask.ca)

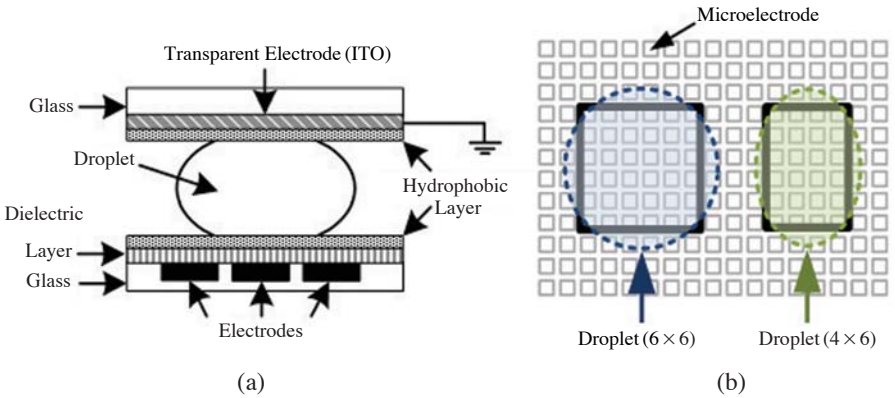

Figure 1. (a) A EWOD-based bi-planar DMFB. (b) Highly customizable configured electrodes in MEDA[5].

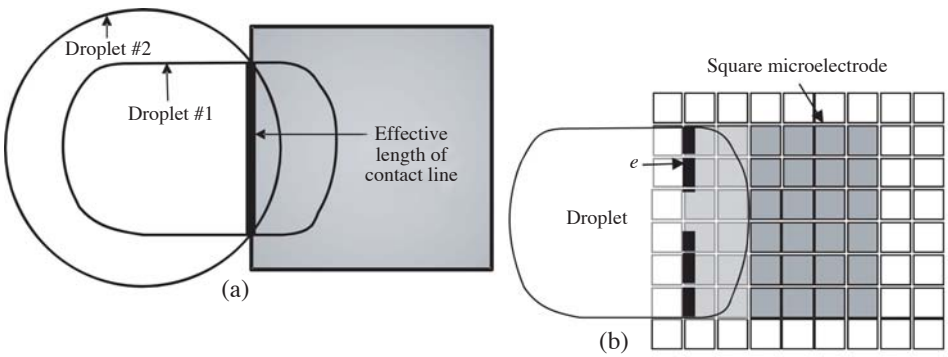

Figure 2. (a) A similar EWOD force on the droplets of different shapes as a result of the same effective length. (b) Effective contact line resulting from square microelectrodes.

ments of multiple variable-sized droplets on a microelectrode array of higher "resolution" (more precise control). The primary goal of this work is to investigate new droplet routing algorithms which can route different sizes of droplets and incorporate diagonal movements and channel-based routing for MEDA architecture.

Microelectrode Dot Array Architecture

Scalability, configurability and portability of fundamental building elements hold the key to the success of hierarchical design of digital microfluidics. To achieve high scalability and configurability of digital microfluidics, the MEDA architecture was proposed based on the concept of "sea-of-microelectrodes array", where an array of identical basic microfluidic components called "microelectrode cells". Unlike other digital microfluidics system where fixed-sized electrodes are arranged in an array or a certain pattern to perform a set of predefined bioassays, a droplet on a MEDA-based DMFB is controlled by a cluster of smaller electrodes called microelectrodes whose sizes can be 10 times smaller than traditional electrodes. Each microelectrode cell consists of a microelectrode and an activation circuit. Similar to a dot-matrix printer, by controlling the associated activation circuit, a MEDA-based DMFB allows dynamic grouping of microelectrodes to form various desired shapes and sizes which can be activated simultaneously to perform microfluidic operations on droplets with different sizes and properties.

Effective length of contact line

Exact modeling and simulations of droplet motion in EWOD is complicated[6]. By careful examination of the MEDA architecture and experimental results, it was found that the magnitude of the EWOD force is primarily determined by the effective length of contact line. As shown in Figure 2(a), the same effective length of two different shapes of droplets results in a similar EWOD force on the individual droplets.

This simplified model indicates the total EWOD force exerted on droplets in MEDA architecture is expected to be reduced as a result of the gaps among microelectrodes. Figure 2(b) shows reduced effective contact line because part of the contact line is located on the gaps among square microelectrodes. The reduced force should be compensated by maximizing the length of the effective contact line at all time. Therefore, in optimizing the performance of EWOD for a MEDA-based DMFB, an electrode should be configured with a cluster of microelectrodes in a way (such as interdigitated electrodes[4]), so that the flexibility of microelectrodes does not adversely affect EWOD operations.

Transportation, merging, mixing, and splitting are four basic droplet operations in a DMFB. Compared to traditional architecture, longer contact line of MEDA allows a number of new approaches to control droplets. Different splitting, merging and mixing operations are also possible with the MEDA architecture. For instance, diagonal splitting can be performed more effectively than the conventional splitting since the surrounding electrodes provide more effective contact lines with the droplet. It is also possible for a mixing module to create multilaminates for fast mixing procedure based on the MEDA architecture. Two droplets are merged at certain area and diagonally split in one direction. Then the droplets are merged again and split in another direction. The above operations are repeated for several times until two droplets are well mixed.

Droplet Routing for MEDA-Based DMFB

Droplet routing is an integral part of DMFB synthesis. A droplet routing problem can be described by a test case which consists of a number of sub-problems. Let $D_i=\{d_1, d_2, ..., d_n\}$ denote a set of droplets in sub-problem S_i. The goal of DMFB droplet routing is to find a path for each droplet in D_i from its source to its designated destination (sink), while minimizing total number of used microelectrode cells, maximum latest arrival time and average latest arrival time in a constrained time. As well, time and fluidic constraints must also be satisfied.

Time constraint

The arrival time for the latest droplet in a sub-problem (i.e. latest arrival time) is not allowed to exceed a certain value. This value is defined as time constraint. In traditional DMFB architecture, it is assumed that a droplet can only move to the adjacent electrode in one time step. In MEDA architecture, however, there are more microelectrodes in a given distance. The time constraint is scaled up by a factor that is proportional to the number of microelectrodes in a configured electrode.

Fluidic constraints

Unlike traditional DMFB, the proposed routing algorithm is for MEDA DMFB architectures, where different sizes of droplets are moved, split, merged, and mixed concurrently. The fluidic constraints are therefore different from other existing droplet routing algorithms. To define droplets with different sizes, the parameters listed below are used (See Figure 3):

1. R is the reference point that indicates the position of a droplet;
2. H and W are height and width of a droplet, respectively;
3. B (bounding width) is the minimum distance between two droplets.

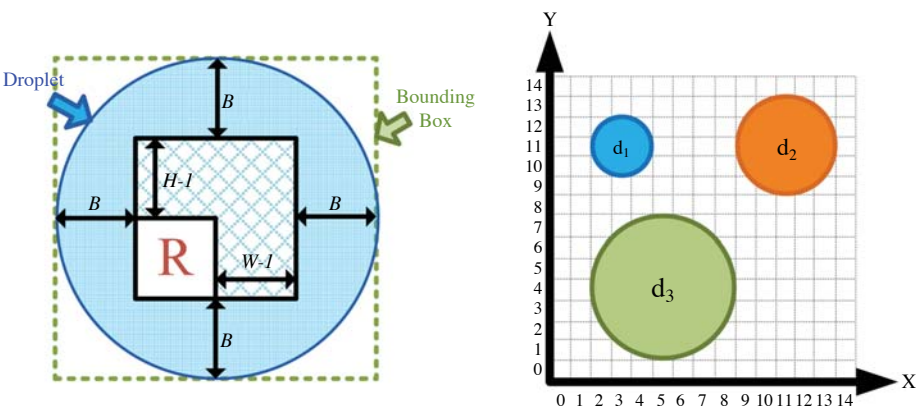

Figure 3. (a) Parameters of a droplet. (b) Different sizes of droplets in MEDA.

The outer box surrounding the droplet is called bounding box. To prevent unwanted mixing, a minimum bounding width of B must be constantly maintained between two droplets during routing. Note that the minimum distance between two droplets is assumed to be the width of one microelectrode cell in this work; i.e., $B=1$.

To simplify the graphic presentation of experiments, the bounding boxes of droplets will not be presented in the rest of figures. For instance, the area of any droplet shown in Figure 3(b) is equivalent to the inner square shaded area in Figure 3(a), but the fluidic constraint among droplets is properly considered in the droplet routing algorithm. The sizes of droplets can be different based on the above definitions as shown in Figure 3(b). For example, d_1 is defined as a 3×3 droplet whose width (W) and height (H) are both equal to 3, while d_2 and d_3 are defined as 5×5 and 7×7 droplets, respectively.

There are two types of fluidic constraints to prevent unwanted mixing. Let (x_i^t, y_i^t), (x_j^t, y_j^t) denotes the positions of droplet d_i and droplet d_j at time step t. These two constraints can be described as follows:

Static constraint
A static constraint defines the minimum distance between droplets at any given time. To prevent this situation, Eq. (1) must be satisfied:

$$|x_i^t-x_j^t|>B+W-1 \text{ or } |y_i^t-y_j^t|>B+H-1 \quad (1)$$

Dynamic constraint
A dynamic constraint defines the minimum distance between droplets at two consecutive time steps. To prevent this situation, Eq. (2) must be satisfied:

$$|x_i^{t+1}-x_j^t|>B+W-1 \text{ or } |y_i^{t+1}-y_j^t|>B+H-1 \quad (2)$$

Results and Discussion

To evaluate the performance of the proposed routing algorithm, a set of test cases were simulated. The effects of diagonal movement, channel-based routing and different sizes of droplets are investigated in terms of maximum latest arrival time, average latest arrival time and total number of used cells. The results with optimal parameters settings are compared with other existing routing algorithms. The conversion equation is given for fair comparison between traditional DMFBs and MEDA.

Criteria

A droplet routing problem can be solved by different routing algorithms. Several criteria are defined to evaluate the quality of a routing algorithm. The first criterion is the total number of used cells. Effective total number of used cells implies reduced contamination area and better fault tolerance. The second criterion is average latest arrival time of a test case. This number represents total amount of time the experiment takes. The third criterion is maximum latest arrival time. Since the traditional architecture and MEDA architecture are different in terms of "resolution", a fair comparison of routing algorithms for these two architecture require appropriate conversions of the resulting total number of used cells, average latest arrival time and maximum latest arrival time.

Conversion of equivalent results

For fair comparison with traditional DMFBs, the results of MEDA are converted to equivalent results using Eqs. (3)-(8). Table 1 shows the notation used in conversion equation. To simplify the routing problem, it is assumed that the width and height of droplet are both equal to W (i.e. $M=N=W$).

The following example shows the equivalent time steps and total number of used cells in a 3×3 channel-based MEDA DMFB. The reference point of droplet is used to indicate the current position of droplet. After the reference point has arrived at the sink, the "tail" of the droplet should also be moved to the sink following the path of reference point. The original time steps can be calculated as $t_{org}^l=t_{eqv}^l\cdot W+W^2-1$. For example, if a 3×3 droplet in MEDA moves for 2 equivalent time steps, the actual (original) time steps used in MEDA are $2\times3+3^2-1=14$. Inferred from the above equation, for channel-based routing results, equivalent maximum latest arrival time and accumulative latest arrival times are calculated by Eqs. (3) and (4); the equivalent total number of used cells is calculated by Eq. (5).

$$t_{eqv}^l=(t_{org}^l+1-W^2)/W \quad (3)$$

$$t_{eqv}^{acc}=(t_{org}^{acc}+1-W^2)/W \quad (4)$$

$$\Omega_{eqv}=\Omega_{org}/W^2 \quad (5)$$

The following example shows the equivalent time

Table 1. Notation used in conversion equations.

Symbol	Explanation
t_{org}^l	Original maximum latest arrival time
t_{org}^{acc}	Original accumulative latest arrival time
Ω_{org}	Original total number of used cells
t_{eqv}^l	Equivalent maximum latest arrival time
t_{eqv}^{acc}	Equivalent accumulative latest arrival time
Ω_{eqv}	Equivalent original total number of used cells
W	Width or height of the droplet

steps and total number of used cells in a 3×3 non-channel-based MEDA DMFB. The original time steps can be calculated as Ω_{org}, inferred from which, for non-channel-based routing results, equivalent maximum latest arrival time and accumulative latest arrival times are calculated according to Eqs. (6) and (7); the equivalent total number of used cells is calculated according to Eq. (8).

$$t^{l}_{eqv} = t^{l}_{org} / W \quad (6)$$

$$t^{acc}_{eqv} = t^{acc}_{org} / W \quad (7)$$

$$\Omega_{eqv} = \Omega_{org} / W^2 \quad (8)$$

Both the Huang's algorithm[7] and the Ho's algorithm[8] show the best results among recent papers. The same benchmark is used to make fair comparison with the proposed work.

Effect of diagonal movement

Significant improvement of diagonal movement can be seen in terms of t^{l}_{eqv}, t^{acc}_{eqv}, and Ω_{eqv} by investigating Table 3 or Table 4. For example, in the optimized results of in-vitro_1 within Table 4, the maximum latest arrival time, average latest arrival time and number of used cells are 18.33, 12.24 and 87.00, respectively. With diagonal movement enabled, these three criteria are improved to 15.33, 9.55 and 64.44. Thus enabling diagonal movement is an efficient approach to take full advantage of MEDA-based DMFBs.

Effect of channel-based routing for MEDA

In non-channel-based routing, as the size of droplets increases, t^{l}_{eqv} and t^{acc}_{eqv} do not change too much, but Ω_{eqv} get increased.

In channel-based routing, t^{l}_{eqv} and t^{acc}_{eqv} get increased compared to non-channel-based routing, but Ω_{eqv} are dramatically reduced. As the size of droplets increases in channel-based routing, t^{l}_{eqv} and t^{acc}_{eqv} increase while get further reduced. This phenomenon can be seen by investigating two cases, in which, the droplet sizes are 2×2 and 3×3, respectively. Both of them move for two equivalent cells. According to Eq. (8), the equivalent used cells of the first case is $2/(2 \times 2) = 0.5$ while the second one is $3/(3 \times 3) = 0.33$. Thus the equivalent cells number decreases as the size of droplets increases.

For some sub-problems such as the one shown in Figure 5(a), enabling channel-based routing also can improve the routability. Since all the test cases used in this work are converted from the test cases used in traditional DMFB architecture, it is unable to show the advantage of improved routability.

Comparision with previous published results

The last row of Table 2, Table 3 and Table 4 compares the results of existing algorithms with our results (optimized 3×3 channel-based MEDA with diagonal movement enabled).

Channel-based routing (Table 4) and non-channel-based routing results (Table 3) are compared to the results in traditional DMFB architecture, respectively.

Table 2. Results of existing works on traditional DMFBs.

BenchMark Suite	Prioritized A*[9]			Two-Stage[10]			Cho's Algorithm[8]			Huang's Algorithm[7]		
Name	Max. A.	Avg. A.	#Cell	Max. A.	Avg. A.	#Cell	Max. A.	Avg. A.	#Cell	Max. A.	Avg. A.	#Cell
in-vitro_1	N/A	N/A	269	N/A	N/A	263	20.00	12.27	292	17.00	9.64	208
in-vitro_2	FAIL	FAIL	FAIL	FAIL	FAIL	FAIL	20.00	10.73	274	15.00	7.80	200
protein_1	FAIL	FAIL	FAIL	N/A	N/A	1735	20.00	15.44	1734	20.00	12.48	1322
protein_2	FAIL	FAIL	FAIL	FAIL	FAIL	FAIL	20.00	9.83	1001	16.00	7.44	718
Avg.	N/A	N/A	N/A	N/A	N/A	N/A	1.29	1.32	4.15	1.10	1.02	3.08

Table 3. Results of 3×3 meda without channel-based routing, D. means diagonal movement is enabled.

BenchMark Suite	Ours (Path-Based), No Channel, 3×3			Ours (Path-Based+D.), No Channel, 3×3			Ours (Optimized), No Channel, 3×3			Ours (Optimized+D.), No Channel, 3×3		
Name	Max. A.	Avg. A.	#Cell	Max. A.	Avg. A.	#Cell	Max. A.	Avg. A.	#Cell	Max. A.	Avg. A.	#Cell
in-vitro_1	23.33	12.73	265.44	17.00	9.67	254.78	17.33	11.79	249.33	15.33	9.30	245.56
in-vitro_2	23.00	11.11	264.89	19.33	8.00	240.44	16.00	10.13	258.44	11.33	7.36	244.44
protein_1	21.67	15.48	1666.56	21.00	12.80	1600.89	21.00	15.27	1614.78	18.67	12.54	1563.00
protein_2	20.00	9.82	967.22	17.33	7.92	909.78	20.00	9.50	940.67	17.33	7.74	893.56
Avg.	1.42	1.34	3.98	1.20	1.05	3.78	1.20	1.27	3.85	1.01	1.01	3.71

Table 4. Results of 3 × 3 meda with channel-based routing, D. means diagonal movement is enabled.

BenchMark Suite	Ours (Path-Based), Channel, 3 × 3			Ours (Path-Based+D.), Channel, 3 × 3			Ours (Optimized), Channel, 3 × 3			Ours (Optimized+D.), Channel, 3 × 3		
Name	Max. A.	Avg. A.	#Cell	Max. A.	Avg. A.	#Cell	Max. A.	Avg. A.	#Cell	Max. A.	Avg. A.	#Cell
in-vitro_1	27.33	13.73	90.00	18.67	9.97	65.33	18.33	12.24	87.00	15.33	9.55	64.44
in-vitro_2	23.00	11.00	91.22	17.00	7.96	66.22	16.00	10.11	85.67	11.33	7.29	64.00
protein_1	26.00	15.81	558.78	23.33	12.80	443.11	21.00	15.24	545.89	18.67	12.30	427.56
protein_2	27.00	10.01	315.56	21.67	7.79	240.78	18.67	9.49	309.44	16.67	7.48	239.11
Avg.	1.67	1.38	1.33	1.30	1.05	1.03	1.19	1.29	1.29	1	1	1

Although Ω_{eqv} can be greatly reduced by increasing droplet size in channel-based routing, t^{l}_{eqv} and t^{acc}_{eqv} are increased as well. Furthermore, non-channel-based routing cannot benefit from the increase of droplet size, either. Thus the results of 3 × 3 (Assumed to be the smallest size of droplet in MEDA in this work) droplet are chosen to make comparison to other's results.

For channel-based routing, it can be seen that t^{l}_{eqv}, t^{acc}_{eqv} and Ω_{eqv} are reduced by enabling channel-based parameter. Especially for Ω_{eqv}, it can be reduced by more than 60% compared to Huang's algorithm. For non-channel-based routing, it concludes that t^{l}_{eqv}, t^{acc}_{eqv} and Ω_{eqv} are reduced slightly. If diagonal movement is enabled, then t^{l}_{eqv} is further decreased.

Conclusions

DMFB systems have been introduced in recent years as an alternative technology of continuous-flow microfluidics biochips. Droplet routing algorithm is a determining factor for effective usage of a DMFB system. This paper presents a new droplet routing algorithm based on 3D-A* search algorithm. To achieve high routability, the algorithm incorporates block setting and dynamic routing. An approach to 3-pin net routing is proposed to avoid undesirable merging during routing. In addition, diagonal movement and an innovative channel-based routing approach are investigated for the MEDA DMFB systems. The simulation results show that diagonal movement is a very effective approach to improve the overall results, while channel-based routing can achieve lower maximum latest arrival time, average latest arrival time and dramatically reduced total number of used cells. The total number of cells is inversely proportional to the size of droplets; i.e. larger droplet size results in reduced cell usage. By enabling channel-based routing, the total number of used cells can be reduced more than 60% compared with the state-of-art works. The comparison further shows that with the channel-based routing disabled, the proposed routing method still results in improved maximum latest arrival time, accumulative latest arrival time and total number of used cells. In summary, the proposed work is the first algorithm that works for both traditional and MEDA architecture without compromising any performance. If the channel-based routing and/or diagonal movement is enabled in MEDA, the routing performance can be significantly improved.

Materials and Methods

3D dynamic-block-based droplet routing method

Since the droplet size may vary in MEDA, the complexity of routing problem increases greatly with the droplet size. For example, if a droplet occupies 7 × 7 microelectrodes and all the droplet sizes are assumed to be same, the size of array changes from M × N to M × N × 7 × 7. Therefore, sequential approach is used in the proposed algorithm, which takes less computation time than concurrent approach such as Integer Linear Programming. In a sequential approach, priority setting and path finding need to be determined respectively. In this section, a path-based priority solver is proposed. In terms of path finding, a block setting algorithm is implemented to apply A* search algorithm to the droplet routing problem. To achieve high routability, a dynamic routing algorithm is applied during routing as well. A new channel-based routing approach for MEDA is also presented.

Priority setting

Typically, prior to solving a sub-problem, a priority solver assigns priorities to individual nets in the sub-problem. The routing algorithm routes each net based on their priorities. Appropriate priority setting is essential to reduction of blockage of lower-priority droplets and prevention of failure of routing. To integrate the priority setting into the proposed routing algorithm, a new priority solver called *path-based priority solver* is proposed for initial priority settings. In this priority solver, each net is routed by a 2D A* search algorithm

without considering other droplets. The following rules are then applied to each net:

1. If a droplet passes through the sources of other droplets, other droplets are assigned with higher priorities.
2. If a droplet passes through the sinks of other droplets, the droplet is assigned with higher priority.

Routing algorithm

Algorithm 1 shows the overall droplet routing algorithm using dynamic routing, where the notations are listed in Table 5. The initial priorities are decided by the path-based priority solver (Algorithm 1, Line 2) based on the two rules as described above (the features of droplets). As the initial priority setting does not always result in 100% routability, the priorities are changed in the proposed dynamic routing approach (Algorithm 1, Line 3 to Line 21). Path finding and block setting algorithm vary with the types of nets (Algorithm 1, Line 7 and Line 9-17).

In the proposed routing algorithm, droplet routing on an electrode array is extended to a 3D space. The x and y axis correspond to the original definition of 2D electrode array. The z axis corresponds to the time steps. The time constraint limits the maximum value of z. Therefore the routing problem can be considered as routing all the nets in a 3D container. Consider a droplet located at (x, y) at time step t, which is represented as (x, y, t). If only vertical and horizontal movements are allowed, there are 5 available positions at the next time step: $(x+1, y, t+1)$, $(x-1, y, t+1)$, $(x, y+1, t+1)$, $(x, y-1, t+1)$ and $(x, y, t+1)$. As MEDA architecture allows diagonal movements, there are four extra available positions at the next time: $(x+1, y+1, t+1)$, $(x+1, y-1, t+1)$, $(x-1, y-1, t+1)$ and $(x-1, y+1, t+1)$.

The fluidic constraints imposed by the bounding width with $B=1$ can be represented by a cube. If a droplet is located at (x, y, t), a $(W+2B) \times (H+2B)$ block cube centered by this droplet cannot be entered by other droplets. If a path is found for a droplet with higher priority, block cubes are generated along this path. Droplets with lower priorities have to avoid entering these block cubes. DMFB routing is similar to a 3D path finding problem. Inspired by the solution to the robot motion planning problem, the proposed routing algorithm applies 3D-A* search algorithm to find the path for each net. There are two major advantages. First, 3D-A* search algorithm is able to route different sizes of droplets in a 3D space, which is important for highly configurable DMFB architecture of MEDA. Secondly, the trend of path and moving directions can be customizable compared to other routing algorithms[7-10].

Table 5. Notation used in the algorithm.

Symbol	Explanation
T_{d_i}	Sink position of d_i
$\hat{T}_{d_i}$	Temporary target position of d_i
c	A microelectrode cell on a microelectrode array
$A_{d_i,c}$	Arrival time of d_i to reach cell c
B_c	The bounding box area of cell c
$\overline{A}$	Time constraint of routing
P_{d_i}	Routed path of d_i
D	Set of droplet
d_i	Droplet i
$\hat{d}_i$	Related droplet of d_i for a 3-pin net
σ	Priority sequence of droplets
π_{d_i}	The priority indicator of droplet d_i
G	A 3D map of DMFB
$\tilde{d}_i$	Pin type of d_i
R	Set of routed paths

Algorithm 1 Overall Algorithm

```
1  begin
2   σ ← apply priority solver based on the features of D
3   repeat
4        D ← sort D in descendent order according to σ
5   foreach d_i in D do
6    if d̃_i ∈ 2-pin
7      P_d̃i ← FindPathAndMarkBlock(d_i, T_di, G)
8    elsif d_i ∈ 3-pin
9      if P_d̂i ≠ φ
10       P_di ← FindPathAndMarkBlock(d_i, T̂_di, G)
11       P_di ← Update path to T_di for d_i
12       P_d̂i ← Update path to T_d̂i for d̂_i
13       MarkBlockForThreePin (P_di, P_d̂i, G)
14     else
15       {T̂_di, T̂_d̂i,} ← Set temporary destinations for d_i and
         d̂_i, respectively
16       P_di FindPathAndMarkBlock (d_i, T̂_di, G)
17     endif
18   endif
19        R ← update P_di
20  endfor
21  until P_di ≠ φ
22  return R
23  end
```

Block setting algorithm

A block is defined as an area that cannot be entered by droplets. In addition to the blocks caused by existing modules on an electrode array, blocks are also generated by the paths of higher priority droplets. A block

setting algorithm, which is also an important part of the routing algorithm, is dependent on the types of nets due to the differences in fluidic constraints for 2-pin and 3-pin nets. To use 3D-A* search algorithm to find a path of each net, a block setting algorithm must consider the types of nets.

Block setting for paths

Figure 4(a) and (b) show the generated blocks by the movement of a droplet in 2D and 3D views. To meet fluidic constraints, block cubes are created along the path of a higher priority droplet so that lower priority droplets are not allowed to enter these areas at specific time steps. Symbol *S* is referred to source and symbol *T* is referred to target hereafter. Note that Figure 4(b) shows the block setting of a 3×3 droplet in MEDA in three time steps, in which, the size of blocks is determined by the size of the droplet.

3D-A* search algorithm is able to automatically handle the stalling operation and some congestions for the low-priority net. Droplets are allowed to share cells at different time steps. For instance, lower priority droplet can pass through shared cells ahead of higher priority droplets; otherwise the lower priority droplet will be moved to a temporary location or wait for a certain time steps until congestion area is freed to pass through. Once a droplet reached its sink, all the 3D block cubes along the path except the sink are marked. For a general droplet, blocks with the same size of the bounding boxes of its sink are generated along the time axis from the arrival time till the end of experiment. For waste droplets, there is no more block after time *t* since they will be moved to a waste reservoir at the sink at time *t*. During routing, a higher priority droplet may pass through the sink of a lower priority droplet. A lower-priority droplet arrived at its sink first may block higher priority droplets. As a result, it is necessary to create a block to prevent the lower priority droplet from entering its sink before higher priority droplets pass through the position.

Block setting for modules

The synthesis stage produces different modules placements for each sub-problem. These modules, existing throughout each experiment, cannot be used for routing. The block setting algorithm generates blocks for these modules from time step 0 to the maximum time step in a 3D space prior to routing.

Net routing

2-pin nets and 3-pin nets need to be processed differently. A 2-pin net, which involves one droplet, defines the source and sink of a droplet. A 3-pin net defines two droplets that need to be merged into a larger droplet for mixing or dilution. Traditionally, one of these two droplets is routed to its sink first, and then the other droplet is routed to the same sink. This approach will move the first droplet out from its sink when the other droplet approaches the sink position. The unnecessary move of the first droplet may cause problem in practical use. A realistic approach to handle 3-pin net is implemented in the proposed routing algorithm. Similar to the traditional approach, the 3-pin net is divided into two 2-pin nets. Instead of routing the two droplets to their common sink sequentially[8], they will be routed to their own temporary destinations which are adjacent to the sink. It should be noted that the priority of these two nets is not necessary in a consecutive order. These two droplets will be merged at the time when the second droplet arrives at its temporary destination, which greatly increases the routing flexibility.

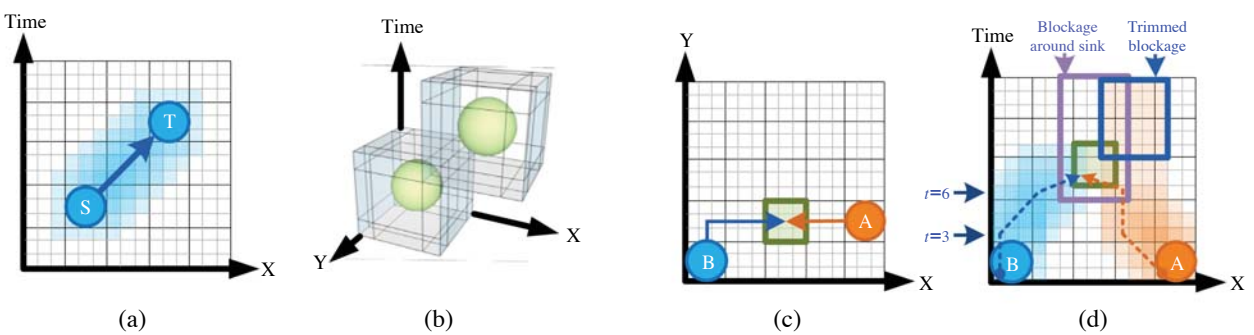

Figure 4. (a) The blocks (shaded area) generated by the movement of a droplet in 2D view. (b) The blocks generated by the movement of a 3×3 droplet in 3D view in three time steps. (c) The block trimming procedure for 3-pin net. d_A will wait until d_B arrives at its own temporary destination. (d) The block trimming procedure for 3-pin net. The dotted line shows the movement paths of the reference points of two droplets.

Block setting algorithm for 3-pin nets requires special care. As illustrated in Figure 4(c) and (d), the first droplet with higher priority is routed to its temporary destination first and generates blocks (shaded area) at this position according to the bounding box. This approach lets the droplet wait for the second droplet to arrive at its own temporary destination without the interruption of irrelevant droplets. When both droplets arrives their temporary destinations, the blocks generated by two droplets around their own temporary destinations are trimmed according to the longer arrival time of two droplets. The two droplets are routed to their common sink at the next time step, which generates a block around the sink. For example, in Figure 4(c) and (d), d_A is routed to its temporary destination first at time t=3 as its priority is higher than d_B, and then blocks on the temporary destination of d_A are generated till the end of experiment. Once d_B is routed to its own temporary destination at time t=6, the longer arrival time A between d_A and d_B is 6. Then the blocks generated on the temporary destination of d_A are modified by trimming the blocks from time t=6. Finally blocks are generated on the common sink of d_A and d_B till the end of experiment.

Dynamic routing

The initial setting of priorities set by the priority solver does not always solve every sub-problem. To resolve this issue, a dynamic routing approach is introduced to adjust the priority during routing. If a net cannot be routed, which implies it is blocked by higher priority nets, this net is set to the highest priority. On the other hand, if a net with the highest priority cannot be routed, the net is set to the lowest priority in order to route other droplets.

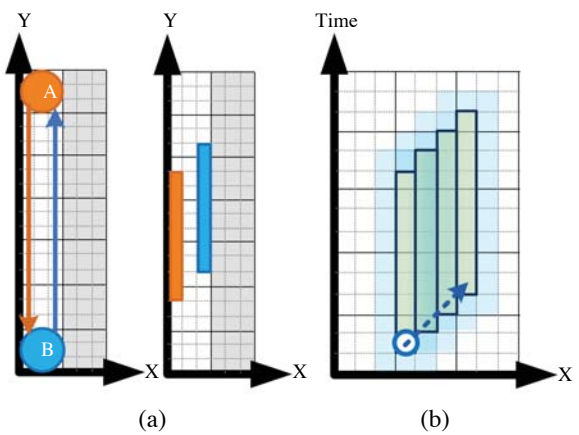

Figure 5. (a) A sub-problem is only routable by channel-based routing in MEDA. (b) Highlighted grids represent the reserved time steps for the "tail" of a 3 × 3 droplet.

Channel-based routing

Thanks to the high configurability of MEDA, an innovative channel-based routing approach is made possible by moving a droplet from its source to a sink through a virtual narrow channel. This approach is able to handle some cases which are unroutable on traditional DMFBs and also effectively avoids the cross contamination as well as reduces total number of used cells.

Figure 5 shows an example that two droplets will switch their positions. The droplets will collide with each other on traditional DMFBs. However, in MEDA DMFB, by enabling the channel-based routing, two droplets are squeezed into two narrow channels and able to reach their sinks without any interference.

In a channel-based routing algorithm, besides finding path for a droplet based on its reference point, a certain number of time steps need to be reserved for the "tail" of droplet, which is shown as the marked area in Figure 5(b). The number of reserved time steps t^{res} for a microelectrode is calculated as $t^{res}=[S_d/S_{ch}]$, in which, S_d is the area of a droplet, and S_{ch} is the area that a droplet can move in one time step. For example, S_d is 9 for a 3 × 3 droplet in Figure 5(b). If a droplet can move only 1 microelectrode in one time step (i.e. S_{ch}=1), the reserved time steps for microelectrode are 9.

Acknowledgements We would like to thank Prof. Tsung-Yi Ho from National Cheng Kung University for providing us with the test cases.

References

1. Whitesides, G. The origins and the future of microfluidics. *Nature* **442**, 368-373 (2006).
2. Chakrabarty, K. Digital Microfluidic Biochips: A Vision for Functional Diversity and More than Moore, presented at the 2010 IEEE Computer Society Annual Symposium on VLSI (ISVLSI) (2010).
3. Cho, S.K., Moon, H. & Kim, C.J. Creating, transporting, cutting, and merging liquid droplets by electrowetting-based actuation for digital microfluidic circuits. *Microelectromechanical Systems, Journal of* **12**, 70-80 (2003).
4. Pollack, M.G., Fair, R.B. & Shenderov, A.D. Electrowetting-based actuation of liquid droplets for microfluidic applications. *Applied Physics Letters* **77**, 96-101 (2000).
5. Wang, G., Teng, D. and Fan, S. Digital microfluidic operations on micro-electrode array architecture, presented at the the 6th IEEE International Conference on Nano/Micro Engineered and Molecular Systems (NEMS) (2011).
6. Young, P.M. & Mohseni, K. Calculation of DEP and

EWOD forces for application in digital microfluidics. *Journal of Fluids Engineering*. **130**, 081603-1~081603-9 (2008).
7. Huang, T. & Ho, T. A fast routability-and performance-driven droplet routing algorithm for digital microfluidic biochips, presented at the 2009 IEEE International Conference on Computer Design (2010).
8. Cho, M. & Pan, D. A high-performance droplet routing algorithm for digital microfluidic biochips. *IEEE Transactions on Computer-Aided Design of Integrated Circuits and Systems* **27**, 1714-1724 (2008).
9. Bohringer, K. Towards optimal strategies for moving droplets in digital microfluidic systems. presented at the 2004 IEEE International Conference on Robotics and Automation (2004).
10. Su, F., Hwang, W. & Chakrabarty, K. Droplet routing in the synthesis of digital microfluidic biochips, presented at the 2006 Design, Automation and Test in Europe (2006).